

The Correspondence Rule for Sonic Logging in Deviated Wells

Douglas E. Miller¹, Steve A. Horne², and John Walsh³

ABSTRACT

For fast anisotropic formations, such as the North American gas shales, sonic logs measure **group slowness** for propagation with the **group angle equal to the borehole inclination angle**. For deviated wells, the distinction between group and phase angle is as important as the distinction between phase and group velocity. When inverting from sonic data to elastic parameters, the use of an incorrect correspondence rule can lead to inconsistent and unrealistic values, particularly for C_{13} or equivalently, Thomsen's δ .

SUMMARY

With increased interest in gas production from shale formations, there has been a corresponding increase in the need to make accurate geophysical measurements of these formations for use in planning and interpreting formation treatments. Because these shale formations are largely composed of microscopically aligned platelets which are also significantly laminated at a macroscale, they are often morphologically anisotropic, with rotational symmetry about a symmetry axis perpendicular to bedding, typically a vertical axis. In such transversely isotropic (VTI) media small perturbations of stress or strain, with respect to a stable reference state, are linearly related via an elastic tensor with five free parameters.

In order to recover elastic parameters from sonic data, one needs a correspondence rule relating velocities $V_l(\psi_{bh})$ extracted from sonic waveforms in a borehole with inclination angle ψ_{bh} to the underlying elastic moduli.

Using the Voigt notation (C_{11} for C_{1111} , C_{13} for C_{1133} , C_{55} for C_{1313} , etc) for elastic moduli, and identifying the

symmetry axis as the (vertical) 3-axis, the density-normalized moduli C_{ij}/ρ have units of velocity squared. Five elastic moduli are required to define VTI anisotropy; these are C_{11} , C_{33} , C_{55} , C_{66} and C_{13} . The first four are related to the squared speeds for wave propagation in the vertical and horizontal directions. $V_{11} = \sqrt{C_{11}/\rho}$ is the wavespeed for horizontally propagating compressional vibration; $V_{66} = \sqrt{C_{66}/\rho}$, the wavespeed for horizontally propagating shear vibration with horizontal polarization; $V_{55} = \sqrt{C_{55}/\rho}$, the wavespeed for vertically propagating shear vibration, as well as for horizontally propagating shear vibration with vertical polarization; $V_{33} = \sqrt{C_{33}/\rho}$, the wavespeed for vertically propagating compressional vibration.

The remaining parameter, C_{13} , cannot be estimated directly, and cannot be estimated at all from measured propagation speeds without either making off-axis measurements or invoking a physical or heuristic model with fewer than five parameters. Nevertheless, accurate measurements of C_{13} are essential for interpreting the results of mini-frac'ing experiments (Thiercelin and Plumb, 1991), for calibrating the relation between sonic measurements and other reservoir characterization measurements (Vernik, 2008), for geomechanical studies (Amadei, 1996; Suarez-Rivera, *et al.*, 2006), and for accurate location of hydrofracture-induced microseismicity (e.g. Warpinski, *et al.*, 2009).

Dipole sonic logs recorded in deviated wells have been used for determination of elastic parameters in a number of studies (e.g. Hornby, *et al.*, 1995; Walsh, *et al.*, 2007). Somewhat surprisingly, there has been a lack of consensus on how the logged sonic wavespeeds are related to the elastic parameters in deviated wells.

Hornby, Howie and Ince (2003) argued that logged compressional speeds were group velocities and found good agreement with field data. Hornby, Wang and Dodds (2003) reported synthetic tests confirming this correspondence rule, concluding '*we are measuring the group velocity for all wave modes excited by the dipole sonic tool.*'

Sinha, *et al.*, (2004) disclosed a variety of ways to de-

¹Department of Earth, Atmospheric, and Planetary Sciences, MIT, formerly Schlumberger-Doll Research, Cambridge MA, USA

²Schlumberger K.K., Fuchinobe, Japan

³Schlumberger DCS, Houston, Texas, USA

rive elastic moduli from logged wavespeeds, based on a weak anisotropy assumption that logged speeds are phase velocities for propagation with phase direction aligned to the borehole axis. Sinha, Simsek and Liu (2006) reported synthetic tests apparently confirming this correspondence rule, concluding ‘*Processing of synthetic waveforms in deviated wellbores using a conventional STC algorithm or a modified matrix pencil algorithm yields phase slownesses of the compressional and shear waves propagating in the nonprincipal directions of anisotropic formations.*’

Thus, there appear to be two conflicting correspondence rules reported in the literature. In point of fact, since the borehole inclination can be matched either to group or phase angle, there are three.

Wavefronts (surfaces of constant traveltime) generated by a point source in a homogeneous anisotropic elastic medium are not in general spherical, leading to two natural notions of “propagation direction” and “propagation speed”. The direction connecting the source to a point on the wavefront is the group (or ray) direction, and apparent speed in this direction is the group (or ray) velocity. The direction normal to the wavefront is the phase (or planewave) direction and apparent speed in this direction is phase velocity.

Mathematically, the relationship between phase and group velocities for VTI anisotropy can be written as

$$v_G^2(\theta) = v_P^2(\theta) + \left[\frac{\partial v_P}{\partial \theta} \right]^2 \quad (1)$$

where θ , the *phase* angle, is the angle of the wavefront normal relative to the symmetry axis, v_P is the plane wave (phase) velocity, and $v_G(\theta)$ is the group (point source) velocity associated with phase angle θ . $\phi = \phi_G(\theta)$, the *group* angle, is the angle of the group velocity vector, relative to the symmetry axis. The two angles satisfy

$$\tan(\theta - \phi_G(\theta)) = \frac{\left[\frac{\partial v_P}{\partial \theta} \right]}{v_P(\theta)} \quad (2)$$

It is of critical importance to distinguish the function v_G which gives group velocity as a function of *phase* angle from the related function v_g which gives group velocity as a function of *group* angle. v_g is typically computed by using (1) and (2), or their equivalents, to calculate both v_G and ϕ_G as functions of phase angle and to iteratively solve or interpolate the equation

$$v_g(\phi_G(\theta)) = v_G(\theta) \quad (3)$$

to determine v_g at arbitrary group angles ϕ .

It follows from the definitions that

$$v_g(\psi_{bh}) \leq v_P(\psi_{bh}) \leq v_G(\psi_{bh}). \quad (4)$$

Moreover, it is a fundamental principle that no energy can propagate in any direction faster than the group velocity in that direction. The introduction of a fluid-filled borehole or other heterogeneity which only supports propagation at slower velocity can only lower the propagation speed.

That is,

$$V_i(\psi_{bh}) \leq v_g(\psi_{bh}). \quad (5)$$

When $v_g(\psi_{bh})$ and $v_P(\psi_{bh})$ are distinct, the logged velocity must be a better approximation to the former than the latter.

For synthetics created with a borehole inclination angle ψ_{bh} , Hornby and his coauthors compared $v_P(\psi_{bh})$ with $v_g(\psi_{bh})$ and determined that the latter gave a better match to $V_i(\psi_{bh})$.

Using synthetic data similar to that of Hornby *et al.*, Sinha and his coauthors compared $v_P(\psi_{bh})$ with $v_G(\psi_{bh})$ and determined that the former gave a better match to $V_i(\psi_{bh})$. That is, in making their comparisons, Sinha, *et al.*, matched the borehole angle to the phase angle rather than to the group angle as Hornby had done. Both of the rules considered by Sinha, *et al.*, are inconsistent with propagation in strongly anisotropic media. Their conclusion that the phase velocity agrees better with the synthetic data than the group velocity is due to their use of $v_G(\psi_{bh})$ with $v_g(\psi_{bh})$.

In weakly anisotropic media, the distinction between $v_P(\psi_{bh})$, $v_G(\psi_{bh})$ and $v_g(\psi_{bh})$ has no practical significance. However, for shales or other strongly anisotropic media, the difference can lead to extreme differences in estimated elastic parameters, particularly for C_{13} .

The present study was motivated by a field example in which sonic data from a pair of wells in a gas shale were remarkably consistent with a single TIV model over a wide range of angles and over all modes of propagation, provided the correct correspondence rule was used. They could not be consistently interpreted using either rule from Sinha, Simsek and Liu (2006). We hope that that example will be released in time to be the main focus of the workshop presentation. For this abstract, we focus on synthetics created to confirm conclusions drawn from the field data and the mathematical observations given above.

Using a 3D finite-difference code developed at the MIT Earth Resources Laboratory (Cheng, 1994), we created a full-waveform synthetic similar to those used by (Hornby *et al.*, 2003) and (Sinha *et al.*, 2006), but based on parameters from our field example. The modeled borehole was inclined at $\psi_{bh} = 55^\circ$ from the vertical symmetry axis.

Figure 1 shows a pressure snapshot at time 1.080 msec (540 timesteps) from the start of the simulation. Overlain are the geometry of the experiment, together with two copies of the analytic wavefront surface for the modeled formation, scaled to represent traveltimes of .813 msec and .693 msec, respectively. Away from the borehole, the shape of the finite-difference wavefront matches the analytic surface, an indication that the source radiates into the solid as an approximate point-source. Near the borehole there is a small distortion of the wavefront shape and a loss of energy to the somewhat complicated reverberant signal in the borehole. In successive snapshots, the pattern moves outward, but does not change, an indication that

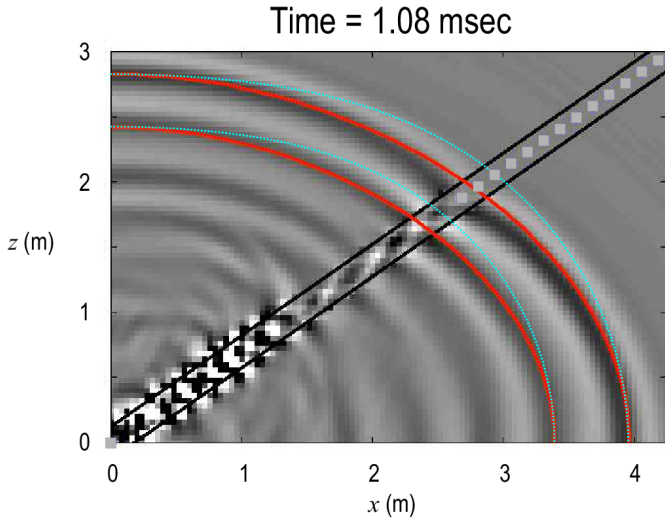


Figure 1: Snapshot of the wavefield at 1.080 milliseconds, overlain by experimental geometry and wavefronts corresponding to the phase (blue dotted line) and group (red continuous line) velocities.

the coupling is at the axial slowness associated with the wavefront in the direction aligned to the borehole. That is, at the group slowness associated with a group angle equal to the borehole inclination angle. Careful observers will note a planewave connecting a bright spot on the borehole wall between the red curves to a point at about 2 m along the horizontal axis. That's a quasi-shear wave whose phase slowness, projected onto the borehole axis matches the group slowness of the qP signal and borehole pressure signal to which it is coupled. There is also some evident direct qSV signal above and below the borehole at about $x = 1.4$ m, $z = 1$ m. A bright Stoneley wave in the borehole is evident starting at about $x = 1$ m, $z = .7$ m.

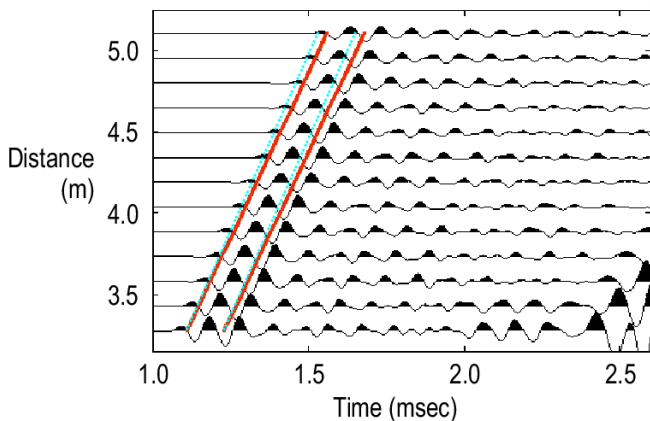


Figure 2: Waveforms overlain by parallel lines corresponding to the phase (blue dotted lines) and group (red continuous lines) velocities from Figure 1.

Figure 2 shows synthetic waveform from thirteen cen-

tered monopole pressure receivers at the locations indicated by gray squares in figure 8. These are spaced to match the tool used to collect our field data. Overlain are two red parallel lines with slope equal to 4.08 m/msec, the group velocity for the modeled formation at group angle equal to ψ_{bh} . Also shown are two blue dotted lines with slopes equal to 4.31 m/msec, the phase velocity for the modeled formation at the phase angle equal to ψ_{bh} . It is evident that the signal is aligned to the group velocity and that, while it has an extended signature, it exhibits no significant temporal dispersion. Sonic modelers will recognize this as 'Partially Transmitted' (PT) compressional signal.

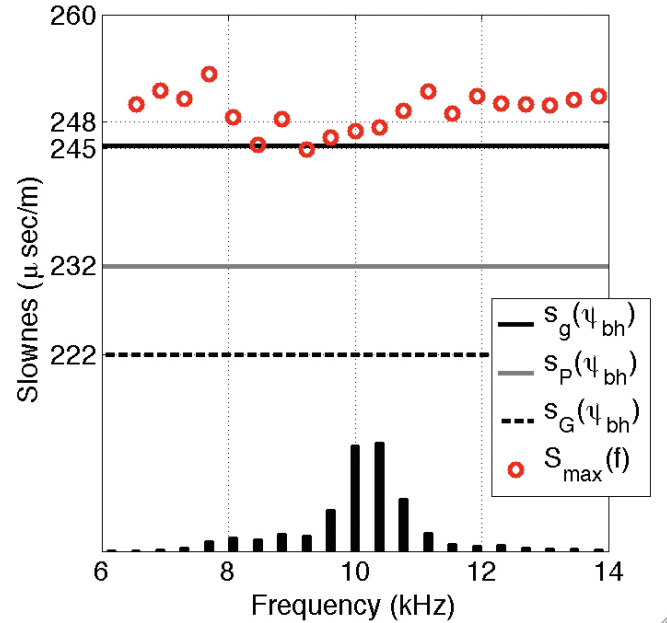


Figure 3: Temporal phase slownesses of the synthetic waveforms.

Figure 3 plots a dispersion analysis for the waveforms from Figure 2, calculated at each frequency, f , as the slowness $S_{max}(f)$ which maximizes semblance at that frequency. We use subscripted s to denote the reciprocal of the corresponding velocity. Thus, for example, the group slowness at phase angle ψ_{bh} is $s_G(\psi_{bh}) = 1/v_G(\psi_{bh})$.

Horizontal lines indicate slownesses $s_G(\psi_{bh}) = 222 \mu\text{sec/m}$, $s_P(\psi_{bh}) = 232 \mu\text{sec/m}$, and $s_g(\psi_{bh}) = 245 \mu\text{sec/m}$, together with the total semblance maximizer $S_{max} = 248 \mu\text{sec/m}$. The extracted slownesses are consistent with our equations (4) and (5) and inconsistent with the interpretation of the measured slowness as either $s_G(\psi_{bh})$ or $s_P(\psi_{bh})$. That is, they are inconsistent with either interpretation matching phase angle to the borehole inclination angle. The semblance max at $248 \mu\text{sec/m}$ is 1% larger than $s_g(\psi_{bh})$, 7% larger than $s_P(\psi_{bh})$, and 12% larger than $s_G(\psi_{bh})$. For comparison, pi is 5% larger than 3.

The bar graph at the bottom of the figure shows a scaled plot of total energy at each frequency. Note that the es-

timated slownesses lie at or above $s_g(\psi_{bh})$. That is, they are at axial wavenumbers that correspond to evanescent qP and oblique outgoing qSV or SH in the solid. This is as expected for PT signal. The decay and small dispersion result from the partial conversion of energy into the transmitted shear modes each time the signal reflects from the fluid/solid boundary. The energy-weighted average of the $S_{max}(f)$ agrees with the global semblance max, S_{max} , to four significant digits.

Standard processing of this data would extract a compressional wavespeed at the semblance max, $S_{max} = 248 \mu\text{sec}/\text{m}$. If this speed is incorrectly interpreted as a measurement of the phase slowness, $s_P(\psi_{bh})$ and substituted as such into the Christoffel equation together with correct values for C_{11} , C_{33} , and C_{55} , a value for C_{13} (or equivalently, Thomsen's δ) is obtained which is far from the correct value and has the wrong sign, i.e., a material with a negative Poisson ratio.

REFERENCES

- Amadei, B., 1996, Importance of anisotropy when estimating and measuring in situ stresses in rock, International Journal of Rock Mechanics and Mining Science and Geomechanics Abstracts, 33 (3) 293-325.
- Cheng, N., 1994, Borehole Wave Propagation in Isotropic and Anisotropic Media: Three-Dimensional Finite Difference Approach, PhD. Thesis, Earth Resources Laboratory, MIT
- Hornby, B., J. Howie, and D. Ince, 2003, Anisotropy correction for deviated-well sonic logs: Application to seismic well tie: Geophysics, 68, 2, 464-471.
- Hornby, B., X. Wang, and K. Dodds, 2003, Do We Measure Phase or Group Velocity with Dipole Sonic Tools?: EAGE, Expanded Abstracts, F29-F29.
- Sinha, B. K., E. Simsek, and Q. H. Liu, 2006, Elastic-wave propagation in deviated wells in anisotropic formations: Geophysics, 71, no. 6, D191-D202.
- Surez-Rivera, R., S. J. Green, J. McLennan, and M. Bai, 2006, Effect of layered heterogeneity on fracture initiation in tight gas shales: SPE paper, 103327.
- Thiercelin, M. J., and R.A. Plumb, 1991, A Core-Based Prediction of Lithologic Stress Contrasts in East Texas Formations: SPE paper 21847.
- Walsh, J., B. Sinha, T. Plona, D. Miller, D. Bentley, and M. Ammerman, 2007, Derivation of anisotropy parameters in a shale using borehole sonic data: SEG Expanded Abstracts, 26, 1, 323-327.
- Vernik, L., 2008, Anisotropic correction of sonic logs in wells with large relative dip: Geophysics, 73, no. 1, E1-E5.
- Warpinski, N. R., C. K. Waltman, J. Du, and Q. Ma, 2009, Anisotropy effects in microseismic monitoring: SPE paper, 124208.